Technical report

Kinematic Analysis of Parallel Spherical Wrist Manipulator

18. 12. 2009

Martin Švejda
msvejda@kky.zcu.cz

Contents

1 Introduction

This report deals with the kinematic analysis of the spherical wrist parallel manipulators. The spherical wrist manipulator (SWM) is often used in an industry as the last part of the industrial manipulators, e.g. SWM is typically mounted on three translation degrees of freedom arm of six degrees of freedom industrial manipulators. The SWM adds three rotation degrees of freedom (e.g. rotation about three axis). From the kinematic viewpoint the SWM can be divided into two main categories - serial SWM and parallel SWM. The examples of these categories are shown in Fig. 1.

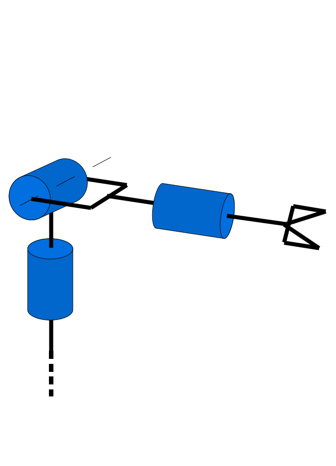

Fig. 1: The left figure: Serial SWM (Actuated revolute joints are blue.) On the right: Parallel SWM (Actuated prismatic joints are blue, black square denotes universal joint, black circle denotes spherical joint.)

The parallel manipulators have a number of advantages in comparison with classical serial manipulators due to their special kinematic architecture, e.g. higher stiffness, higher accuracy,lower moving mass, and so on. On the other hand there are some drawbacks which complicate the design of the parallel manipulators, e.g. more complex kinematic structure, more complex input-output relationship[1], an irregular shape of the workspace. These drawbacks make the design of the parallel manipulators more difficult contrary of their serial counterparts. Many of the examples of the parallel kinematic architectures may be find in [4].

2 Kinematics of parallel SWM

The parallel SWM is shown in Fig. 2. It consists of three independent kinematic chains which are mounted to the base by the weld joints and to the end-effector by the spherical joints. Two links of each kinematic chain is connected by the universal joint. The parallel SWM is actuated by three prismatic actuators (actuated prismatic joints). Passive stabilization element ensures three rotation degrees of freedom of the end-effector of the parallel SWM. Because the actuators of the parallel SWM are rigidly mounted on the base the proposed architecture is suitable for applications in which we require:

- Very fast motion of the end-effector (low motion mass).

[1]Relationship between the joint coordinates and the generalized coordinates (end-effector coordinates).

- The end-effector is supposed to work within a dangerous area (e.g. high temperature, aggressive and combustive spaces and so on) because the actuators can be easily separated from these area.

Let $\Theta = \begin{bmatrix} l_1 & l_2 & l_3 \end{bmatrix}^T = \begin{bmatrix} \|\overrightarrow{B_1C_1}\| & \|\overrightarrow{B_2C_2}\| & \|\overrightarrow{B_3C_3}\| \end{bmatrix}^T$ denotes actuated joint coordinates and $X = \begin{bmatrix} \alpha & \beta & \gamma \end{bmatrix}^T$ denotes generalized end-effector coordinates where α, β, γ are XYZ Euler's angles representing the consecutive rotation of the end-effector about X-axis, Y-axis and Z-axis. The set of the design parameters of the parallel SWM is given by the vector $\xi = \begin{bmatrix} a_1 & a_2 & l & l_0 \end{bmatrix}^T$ where a_1, a_2 are lengths of the sides of equilateral triangles representing the base and end-effector consequently, l is a length of the links connecting prismatic actuators to the end-effector and l_0 is a length of the prismatic actuators at the parallel SWM's home position ($\alpha = \beta = \gamma = 0$).

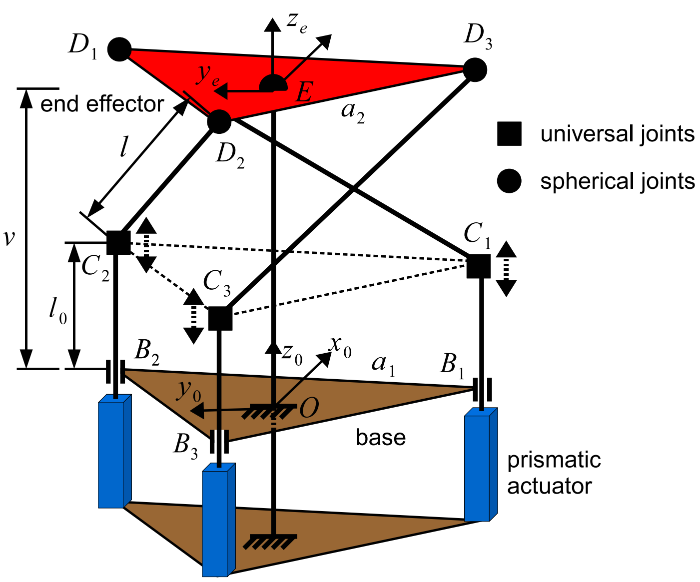

Fig. 2: Scheme of the parallel SWM in a home position

2.1 Inverse kinematic problem

Inverse kinematic problem (IKP) involves finding a mapping from the generalized end-effector coordinates X to the actuated joint coordinates Θ.

We denote $O - x_0y_0z_0$ to be the base coordinate system with the origin in the center of mass of the base's equilateral triangle and $E - x_ey_ez_e$ to be the end-effector coordinate system with the origin in the center of mass of the end-effector's equilateral triangle. The end-effector orientation can be expressed by the rotation matrix[2] R_e^0 which consist of the elementary rotations matrix about X, Y and Z axis by the angles α, β, γ.

$$R_e^0 = R_e^0(X) = R_1(\alpha) \cdot R_2(\beta) \cdot R_3(\gamma) =$$
$$= \begin{bmatrix} 1 & 0 & 0 \\ 0 & \cos(\alpha) & -\sin(\alpha) \\ 0 & \sin(\alpha) & \cos(\alpha) \end{bmatrix} \cdot \begin{bmatrix} \cos(\beta) & 0 & \sin(\beta) \\ 0 & 1 & 0 \\ -\sin(\beta) & 0 & \cos(\beta) \end{bmatrix} \cdot \begin{bmatrix} \cos(\gamma) & -\sin(\gamma) & 0 \\ \sin(\gamma) & \cos(\gamma) & 0 \\ 0 & 0 & 1 \end{bmatrix} \quad (1)$$

[2] R_e^0 denotes the rotation matrix of coordinate system $E - x_ey_ez_e$ with respect to the coordinate system $O - x_0y_0z_0$ and e.g. B_1^0 denotes the coordinates of the B_1 point with respect to the coordinate system $O - x_0y_0z_0$.

It is clear that the vertices of the equilateral triangles representing the base and the end-effector respectively are

$$B_1^0 = \begin{bmatrix} \frac{\sqrt{3}}{6}a_1 & -\frac{1}{2}a_1 & 0 \end{bmatrix}^T, \; B_2^0 = \begin{bmatrix} \frac{\sqrt{3}}{6}a_1 & \frac{1}{2}a_1 & 0 \end{bmatrix}^T, \; B_3^0 = \begin{bmatrix} -\frac{\sqrt{3}}{3}a_1 & 0 & 0 \end{bmatrix}^T \tag{2}$$

with respect to the coordinate system $O - x_0y_0z_0$ and

$$D_1^e = \begin{bmatrix} \frac{\sqrt{3}}{6}a_2 & \frac{1}{2}a_2 & 0 \end{bmatrix}^T, \; D_2^e = \begin{bmatrix} -\frac{\sqrt{3}}{3}a_2 & 0 & 0 \end{bmatrix}^T, \; D_3^e = \begin{bmatrix} \frac{\sqrt{3}}{6}a_2 & -\frac{1}{2}a_2 & 0 \end{bmatrix}^T \tag{3}$$

with respect to the coordinate system $E - x_ey_ez_e$.

The end-effector is connected to the base by three actuated independent serial kinematic chains[3] $B_i\,C_i\,D_i$ where $i = 1, 2, 3$. Let v is a high of the parallel SWM then the translation vector between coordinates system $O - x_0y_0z_0$ and $E - x_ey_ez_e$ is $\overrightarrow{OE}^0 = \begin{bmatrix} 0 & 0 & v \end{bmatrix}^T$.

The vectors $\overrightarrow{B_iD_i}^0$ can be written as

$$\overrightarrow{B_iD_i}^0 = \overrightarrow{B_iD_i}^0(X) = \overrightarrow{B_iO}^0 + \overrightarrow{OE}^0 + R_e^0\,\overrightarrow{ED_i}^e, \tag{4}$$

where

$$\overrightarrow{B_iO}^0 = -B_i^0, \quad \overrightarrow{ED_i}^e = D_i^e$$

We define the function $\mathbf{H_1}(X)$ as

$$\mathbf{H_1}(X) = \begin{bmatrix} \overrightarrow{B_1D_1}^0 \\ \overrightarrow{B_2D_2}^0 \\ \overrightarrow{B_3D_3}^0 \end{bmatrix} = \begin{bmatrix} \overrightarrow{B_1O}^0 + \overrightarrow{OE}^0 + R_e^0\,\overrightarrow{ED_1}^e \\ \overrightarrow{B_2O}^0 + \overrightarrow{OE}^0 + R_e^0\,\overrightarrow{ED_2}^e \\ \overrightarrow{B_3O}^0 + \overrightarrow{OE}^0 + R_e^0\,\overrightarrow{ED_3}^e \end{bmatrix}, \tag{5}$$

which is a vector function of dimension 9 in 3 variables (X).

Then the actuated joint coordinates Θ are found for each of these independent kinematic chains as an inverse kinematic problem of serial manipulators [1].

We denote for i-th serial kinematic chain $B_i\,C_i\,D_i$ that the vector $\overrightarrow{B_iD_i}^0$ is a position (generalized coordinates) of the chain's end-effector, ϑ_i^x and ϑ_i^y are XY Euler angles representing the consecutive rotation of the link C_iD_i about X-axis, Y-axis with respect to the base coordinate system. Then the forward kinematic problem[4] for i-th serial kinematic chain $B_i\,C_i\,D_i$ can be formulated as follows

$$\overrightarrow{B_iD_i}^0 = \overrightarrow{B_iD_i}^0(l_i, \vartheta_i^x, \vartheta_i^y) = \overrightarrow{u_i}^0 \cdot l_i + \bar{R}_i^0 \cdot \overrightarrow{u_i}^0 \cdot l, \tag{6}$$

where $\overrightarrow{u_i}^0 = \overrightarrow{B_iC_i}^0 / \|\overrightarrow{B_iC_i}^0\|$ is a direction vector of the prismatic actuators with respect to the base coordinate system and

$$\bar{R}_i^0 = \begin{bmatrix} 1 & 0 & 0 \\ 0 & \cos\vartheta_i^x & -\sin\vartheta_i^x \\ 0 & \sin\vartheta_i^x & \cos\vartheta_i^x \end{bmatrix} \cdot \begin{bmatrix} \cos\vartheta_i^y & 0 & \sin\vartheta_i^y \\ 0 & 1 & 0 \\ -\sin\vartheta_i^y & 0 & \cos\vartheta_i^y \end{bmatrix}$$

is a rotation matrix with respect to the base coordinate system.

Let we suppose a new vector of the joint coordinates

$$\bar{\Theta} = \begin{bmatrix} \Theta \\ \Theta_P \end{bmatrix}, \tag{7}$$

[3] Serial kinematic chain = serial manipulator.
[4] For explanation, see section 2.4.

where $\Theta = \begin{bmatrix} l_1 & l_2 & l_3 \end{bmatrix}^T$ are the well-known actuated joint coordinates and $\Theta_P = \begin{bmatrix} \vartheta_1^x & \vartheta_1^y & \vartheta_2^x & \vartheta_2^y & \vartheta_3^x & \vartheta_3^y \end{bmatrix}^T$ are the passive joint coordinates.

We define the function $\mathbf{H_2}(\bar{\Theta})$ as

$$\mathbf{H_2}(\bar{\Theta}) = \begin{bmatrix} \overrightarrow{B_1 D_1}^0 \\ \overrightarrow{B_1 D_2}^0 \\ \overrightarrow{B_1 D_3}^0 \end{bmatrix} = \begin{bmatrix} \overrightarrow{u_1}^0 \cdot l_1 + \bar{R}_1^0 \cdot \overrightarrow{u_1}^0 \cdot l \\ \overrightarrow{u_2}^0 \cdot l_2 + \bar{R}_2^0 \cdot \overrightarrow{u_2}^0 \cdot l \\ \overrightarrow{u_3}^0 \cdot l_3 + \bar{R}_3^0 \cdot \overrightarrow{u_3}^0 \cdot l \end{bmatrix} \tag{8}$$

which is a vector function of dimension 9 in 9 variables ($\bar{\Theta}$).

If we fixed the general coordinates X to be constant and equate (5) to (8) we obtain the system of 9 equations in 9 variables ($\bar{\Theta}$) which solves the inverse kinematic problem of the parallel SWM and gives us the relationship between the actuated and passive joint coordinates which is independent of X.

It is worth noticing that the solution can be very complex namely for serial kinematic chains with complicated forward kinematics. In practise we often need not to know complete inverse kinematic mapping of the parallel SWM in means of $X \to \bar{\Theta}$ but only the relationship between actuated joint coordinates Θ and generalized coordinates X in means of $X \to \Theta$. In this case the inverse kinematic problem of the i-th serial kinematic chain can be simplify by the following consideration.

If we denote the known vector in (4) as $\overrightarrow{BD_i}^0 = \begin{bmatrix} d_{ix} & d_{iy} & d_{iz} \end{bmatrix}^T$ then the constant length vector $\overrightarrow{C_i D_i}^0$ can be expressed (for a choice of $\overrightarrow{u_i}^0 = \begin{bmatrix} 0 & 0 & 1 \end{bmatrix}^T$) as

$$\overrightarrow{C_i D_i}^0 = \begin{bmatrix} d_{ix} & d_{iy} & d_{iz} - l_i \end{bmatrix}^T \tag{9}$$

Consequently

$$\begin{aligned} \|\overrightarrow{C_i D_i}^0\|^2 &= d_{ix}^2 + d_{iy}^2 + (d_{iz} - l_i)^2 = l^2 \\ (d_{iz} - l_i)^2 &= l^2 - d_{ix}^2 - d_{iy}^2 \\ d_{iz} - l_i &= \pm\sqrt{l^2 - d_{ix}^2 - d_{iy}^2} \\ l_i &= d_{iz} \mp \sqrt{l^2 - d_{ix}^2 - d_{iy}^2}, \end{aligned} \tag{10}$$

where

$$d_{ix} = d_{ix}(X), \quad d_{iy} = d_{iy}(X), \quad d_{iz} = d_{iz}(X)$$

We can see that inverse kinematic mapping (10) has a real solution if and only if $l^2 \geq d_{ix}^2 + d_{iy}^2$. A real solution of (10) means that the parallel SWM can be assembled for the given orientation X of the end-effector.

The relationship between the design parameter l_0 and high v is obtained analogously as in the equations (4, 9, 10) if we suppose that the parallel SWM is in a home position ($l_i = l_0, \alpha = \beta = \gamma = 0 \Rightarrow R_e^0 = I$).

$$v = l_0 \pm \sqrt{l^2 - k_1^2 - k_2^2}, \tag{11}$$

where

$$k_1 = \frac{\sqrt{3}}{6}(a_2 - a_1), \quad k_2 = \frac{1}{2}(a_1 + a_2)$$

For given size of the base a_1, end-effector a_2 and length l the equation (11) shows that the high of the parallel SWM is linearly dependent on the design parameter l_0.

The equation (11) has a real solution if and only if $l^2 \geq k_1^2 + k_2^2$. This inequality plays a crucial role in a design of the parallel SWM and ensures that it can be assembled (for given design parameters ξ) in a home position.

The final inverse kinematic mapping of the parallel SWM for given design parameters ξ is given by the equation (11) and (10) and has two real solutions. The inverse kinematic mapping may be written shortly as $\Theta = G(X, \xi)$. The simulation model of the parallel SWM is established in Matlab/Simulink/SimMechanics [2]. Fig. 3 shows two solutions of the inverse kinematic problem of the parallel SWM in a home position.

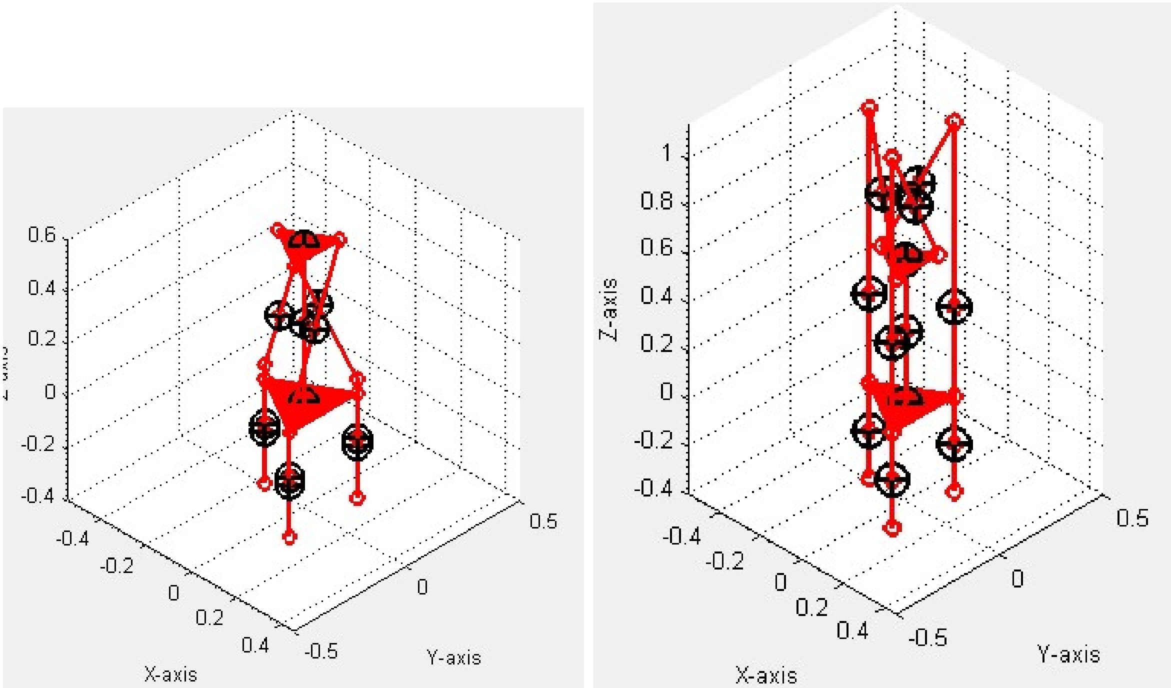

Fig. 3: Two solutions of the inverse kinematic problem of the parallel SWM

Hereafter we suppose only the solution of the inverse kinematic problem where the end-effector is placed above the base. Fig. 4 shows different postures of the end-effector.

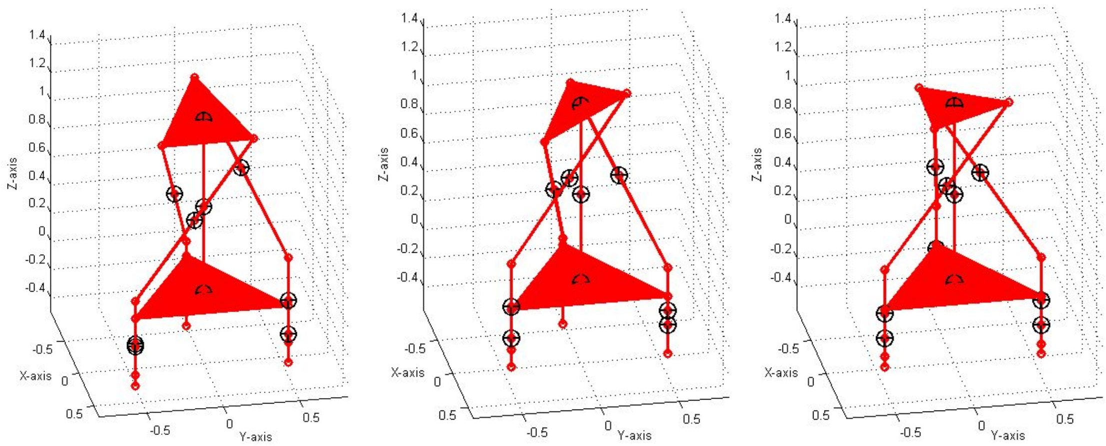

(a) $\alpha = 0.5$, $\beta = \gamma = 0$ (b) $\beta = 0.5$, $\alpha = \gamma = 0$ (c) $\gamma = 0.5$, $\alpha = \beta = 0$

Fig. 4: Different postures of the parallel SWM

2.2 Differential kinematics

The differential kinematic mapping gives the relationship between the actuated joint velocities $\frac{d}{dt}\Theta = \begin{bmatrix} \frac{d}{dt}l_1 & \frac{d}{dt}l_2 & \frac{d}{dt}l_3 \end{bmatrix}^T$ and the generalized end-effector velocities $\frac{d}{dt}X = \begin{bmatrix} \frac{d}{dt}\alpha & \frac{d}{dt}\beta & \frac{d}{dt}\gamma \end{bmatrix}^T$ (or $\omega = \begin{bmatrix} \omega_x & \omega_y & \omega_z \end{bmatrix}^T$, see Note 1). From Fig. 2 it is clear that the length l of the link $\overrightarrow{C_iD_i}$ [5] is constant and it leads to

$$|\overrightarrow{C_iD_i}|^2 = \overrightarrow{C_iD_i}^T \cdot \overrightarrow{C_iD_i} = l^2 \tag{12}$$

By differentiating this equation with respect to time we get[6]

$$2\left(\overrightarrow{C_iD_i}\,,\, \frac{d}{dt}\overrightarrow{C_iD_i}\right) = 0 \tag{13}$$

The time derivative of the vector $\overrightarrow{C_iD_i}$ is given by the difference

$$\frac{d}{dt}\overrightarrow{C_iD_i} = v_{D_i} - v_{C_i} = \omega \times \overrightarrow{ED_i} - \frac{d}{dt} \cdot \overrightarrow{u_i} \tag{14}$$

where v_{D_i} is the velocity of the D_i point, v_{C_i} is the velocity of the C_i point, $\omega = \begin{bmatrix} \omega_x & \omega_y & \omega_z \end{bmatrix}^T$ is the end-effector velocity vector with respect to the base coordinate system.

■ **Note 1 (Euler's kinematic equations)**
The time derivatives of the XYZ Euler angles $\frac{d}{dt}X = \begin{bmatrix} \frac{d}{dt}\alpha & \frac{d}{dt}\beta & \frac{d}{dt}\gamma \end{bmatrix}^T$ are related to the end-effector velocity vector $\omega = \begin{bmatrix} \omega_x & \omega_y & \omega_z \end{bmatrix}^T$ by the so-called *Euler's kinematic equations* as it is shown in [1].

$$\begin{bmatrix} \omega_x \\ \omega_y \\ \omega_z \end{bmatrix} = \begin{bmatrix} \frac{d}{dt}\alpha + \frac{d}{dt}\gamma \cdot \sin\beta \\ -\cos\beta \cdot \frac{d}{dt}\gamma \cdot \sin\alpha + \frac{d}{dt}\beta \cdot \cos\alpha \\ \cos\beta \cdot \cos\alpha \cdot \frac{d}{dt}\gamma + \sin\alpha \cdot \frac{d}{dt}\beta \end{bmatrix} \tag{15}$$

$$\omega = H(X) \cdot \frac{d}{dt}X, \tag{16}$$

where

$$H(X) = \begin{bmatrix} 1 & 0 & \sin\beta \\ 0 & \cos\alpha & -\sin\alpha\cos\beta \\ 0 & \sin\alpha & \cos\alpha\cos\beta \end{bmatrix}$$

■

Substituting (14) to (13) we get

$$\left(\overrightarrow{C_iD_i}\,,\, \omega \times \overrightarrow{ED_i} - \frac{d}{dt}l_i \cdot \overrightarrow{u_i}\right) = 0$$

$$\left(\omega \times \overrightarrow{ED_i}\,,\, \overrightarrow{C_iD_i}\right) - \left(\overrightarrow{C_iD_i}\,,\, \overrightarrow{u_i}\right) \cdot \frac{d}{dt}l_i = 0$$

$$\left(\omega\,,\, \overrightarrow{ED_i} \times \overrightarrow{C_iD_i}\right) - \left(\overrightarrow{C_iD_i}\,,\, \overrightarrow{u_i}\right) \cdot \frac{d}{dt}l_i = 0$$

$$\frac{\left(\omega\,,\, \overrightarrow{ED_i} \times \overrightarrow{C_iD_i}\right)}{\left(\overrightarrow{C_iD_i}\,,\, \overrightarrow{u_i}\right)} = \frac{d}{dt}l_i, \tag{17}$$

[5]Hereafter, the superscript "0" is omitted for terms referred to the base coordinate system $O - x_0y_0z_0$.
[6]$(x\,,\,y)$ denotes a *dot product* of the vector x and y.

where the vectors $\overrightarrow{ED_i}$ and $\overrightarrow{C_iD_i}$ depend on the given posture X of the parallel SWM.

$$\overrightarrow{ED_i} = R_e \cdot \overrightarrow{ED_i}^e$$
$$\overrightarrow{C_iD_i} = D_i - C_i = \overrightarrow{OE} + R_e \cdot \overrightarrow{ED_i}^e - \left(\overrightarrow{OBi} + l_i \cdot \overrightarrow{u_i}\right)$$

The equation (17) for $i = 1,\, 2,\, 3$ gives a differential kinematic mapping which can be written as follows

$$\frac{d}{dt}\Theta = J_k^{-1}\left(X\right) \cdot \omega \tag{18}$$

or

$$\frac{d}{dt}\Theta = J^{-1}\left(X\right) \cdot \frac{d}{dt}X, \tag{19}$$

where

$$J_k^{-1}\left(X\right) = \begin{bmatrix} \frac{\left(\overrightarrow{ED_1}\times\overrightarrow{C_1D_1}\right)^T}{\left(\overrightarrow{C_1D_1}\,,\overrightarrow{u_1}\right)} \\ \cdots\cdots\cdots\cdots \\ \frac{\left(\overrightarrow{ED_2}\times\overrightarrow{C_2D_2}\right)^T}{\left(\overrightarrow{C_2D_2}\,,\overrightarrow{u_2}\right)} \\ \cdots\cdots\cdots\cdots \\ \frac{\left(\overrightarrow{ED_3}\times\overrightarrow{C_3D_3}\right)^T}{\left(\overrightarrow{C_3D_3}\,,\overrightarrow{u_3}\right)} \end{bmatrix} \qquad (\textit{inverse kinematic jacobian})$$

$$J^{-1}\left(X\right) = J_k^{-1}\left(X\right) \cdot H\left(X\right) \qquad (\textit{inverse jacobian})$$

2.3 Singularities

Singularity positions are particular positions of a manipulator for which a manipulator loses its inherent rigidity and for which the end-effector will have uncontrollable degrees of freedom. The relationship (18) between the actuated joint velocities and end-effector velocity vector can be rewritten as

$$J_k^{-1}(X) = A(X)^{-1} \cdot B(X) \quad \Rightarrow \quad A(X) \cdot \frac{d}{dt}\Theta = B(X) \cdot \omega, \tag{20}$$

where

$$A(X) = \begin{bmatrix} \left(\overrightarrow{C_1D_1}\,,\, \overrightarrow{u_1}\right) & 0 & 0 \\ 0 & \left(\overrightarrow{C_2D_2}\,,\, \overrightarrow{u_2}\right) & 0 \\ 0 & 0 & \left(\overrightarrow{C_3D_3}\,,\, \overrightarrow{u_3}\right) \end{bmatrix} \quad \text{and} \quad B(X) = \begin{bmatrix} \left(\overrightarrow{ED_1} \times \overrightarrow{C_1D_1}\right)^T \\ \cdots\cdots\cdots\cdots \\ \left(\overrightarrow{ED_2} \times \overrightarrow{C_2D_2}\right)^T \\ \cdots\cdots\cdots\cdots \\ \left(\overrightarrow{ED_3} \times \overrightarrow{C_3D_3}\right)^T \end{bmatrix} \tag{21}$$

It can be seen that elements of the matrix $A(X)$ and $B(X)$ are bounded by the means of the definition of a dot product and a vector product. Let a_{ii} and b_{ij} for $i = 1,\, 2,\, 3;\ j = 1,\, 2,\, 3$ are the elements of the matrix $A(X)$ and $B(X)$ respectively and consider an absolute value of the dot product of two vectors U a V to be $\|\left(U\,,\,V\right)\| = \|U\| \cdot \|V\| \cdot \|\cos\alpha\|$ and a norm of the cross product of two vectors U a V to be $\|U \times V\| = \|U\| \cdot \|V\| \cdot \sin\alpha$, where $\alpha \in \langle 0,\, \pi\rangle$ is the angle between U and V. Then the following holds for the elements of the matrix $A(X)$

$$\|a_{ii}\| = \|\left(\overrightarrow{C_iD_i}\,,\, \overrightarrow{u_i}\right)\| \leq \|\overrightarrow{C_iD_i}\| \cdot \underbrace{\|\overrightarrow{u_i}\|}_{=1}, \tag{22}$$

and for the elements of the matrix $B(X)$

$$\begin{aligned} b_{i1}^2 + b_{i2}^2 + b_{i3}^2 \leq \|\overrightarrow{ED_i}\|^2 \cdot \|\overrightarrow{C_iD_i}\|^2 \\ \Rightarrow \|b_{i1}\| \leq \|\overrightarrow{ED_i}\| \cdot \|\overrightarrow{C_iD_i}\|,\ \|b_{i2}\| \leq \|\overrightarrow{ED_i}\| \cdot \|\overrightarrow{C_iD_i}\|,\ \|b_{i3}\| \leq \|\overrightarrow{ED_i}\| \cdot \|\overrightarrow{C_iD_i}\|, \end{aligned} \tag{23}$$

where the constants $\|C_iD_i\|$ and $\|ED_i\|$ are given by the design parameters ξ of the parallel SWM.

In such a way we can distinguish 3 types of singularities:

- The matrix $A(X)$ is singular $\Rightarrow$ *serial singularity.* This type of singularity means that there will exist nonzero actuated joint velocity vector $\frac{d}{dt}\Theta$ for which the end-effector cannot move ($\omega = \overrightarrow{0}$). It is very often claimed that this type of singularity corresponds to so-called workspace limit for which the end-effector cannot move too, but it is not true. For the parallel SWM holds that the serial singularity occurs only for the vectors $\overrightarrow{C_iD_i}$ and $\overrightarrow{u_i}$ that are perpendicular to each other.
- The matrix $B(X)$ is singular $\Rightarrow$ *parallel singularity.* This type of singularity means that there will exist nonzero end-effector velocity vector ω for which the actuated joints do not move ($\frac{d}{dt}\Theta = \overrightarrow{0}$). For the parallel SWM holds that this type of singularity occurs only if at least one of the vectors $\overrightarrow{ED_i} \times \overrightarrow{C_iD_i}$ is a zero vector ($\overrightarrow{ED_i}$ and $\overrightarrow{C_iD_i}$ are parallel to each other) or if the vectors $\overrightarrow{ED_i} \times \overrightarrow{C_iD_i}$ are linearly dependent. For an example, see Fig. 5
- The matrices $A(X)$ and $B(X)$ are singular. The end-effector can move when the actuators are locked and vice versa. For an example, see Fig. 6

The parallel singularities of the manipulators play crucial role in a design and control because these type of singularities not only lead to uncontrolled degrees of freedom of the end-effector but application of a *principle of virtual work* allows to determine the relationship between actuated joint forces and end-effector forces (torques) when the manipulator is at the equilibrium position[7].

Let τ denotes the vector of actuated joint forces and F denotes the vector of end-effector torques the elementary work associated with them may be written (with consideration of (18))

$$dW_\tau = \tau^T \cdot d\Theta = \tau^T \cdot J_k^{-1} \cdot \omega dt \tag{24}$$

$$dW_X = F^T \cdot \omega dt \tag{25}$$

where $d\Theta$ is an elementary displacement of the actuators and ωdt is an elementary rotation of the end-effector.

According to the principle of virtual work the following holds for the manipulator at the equilibrium position

$$\begin{aligned} dW_\tau &= dW_X \\ \tau^T \cdot J_k^{-1} \cdot \omega dt &= F^T \cdot \omega dt \\ J_k^{-T} \cdot \tau &= F \end{aligned} \tag{26}$$

The relationship (26) implies that the actuated joint forces can become very large for relatively small values of the end-effector torques if the robot is on a neighbourhood of the parallel singular position (J_k^{-1} is singular). This can lead to damage of the manipulator. For an example if we will force the end-effector by the torque 0.1 [Nm] about z-axis ($F = \begin{bmatrix} 0 & 0 & 0.1 \end{bmatrix}^T$) the actuated

[7] The manipulator does not move and there are not any forces of gravity affecting the manipulator.

joint forces on a neighbourhood of parallel singular position ($X = \left[\begin{array}{ccc} 0 & 0 & (\frac{1}{3}\pi + 0.02) \end{array}\right]^T$) will be $\tau \doteq \left[\begin{array}{ccc} 77 & 77 & 77 \end{array}\right]^T$ [N].

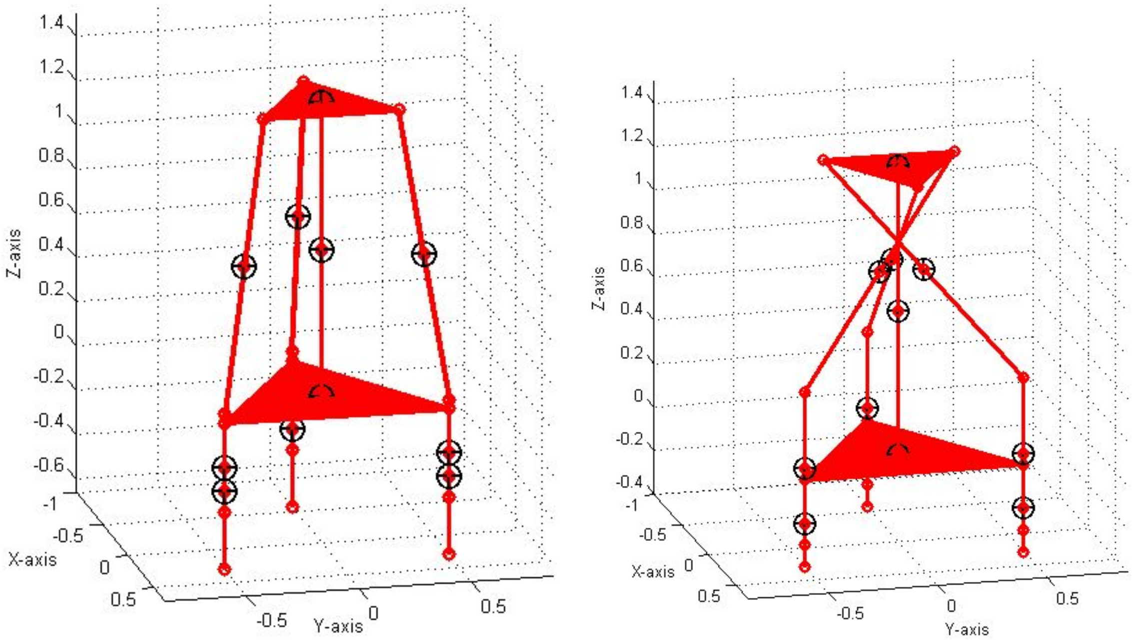

(a) $\alpha = \beta = 0$, $\gamma = -\frac{2}{3}\pi$ (b) $\alpha = \beta = 0$, $\gamma = \frac{1}{3}\pi$

Fig. 5: Examples of the parallel singular positions of the parallel SWM

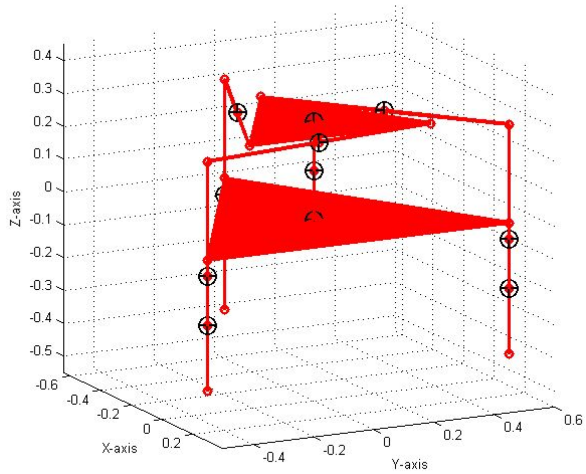

Fig. 6: Examples of the parallel and serial singular position of the parallel SWM ($\alpha = \beta = \gamma = 0$, the design parameters are different from the previous examples)

2.4 Forward kinematic problem

Forward kinematic problem (FKP) involves finding a mapping from the actuated joint coordinates Θ to the generalized end-effector coordinates X. Note, that the inverse kinematic mapping given by

$$\Theta = G(X,\ \xi) \tag{27}$$

is complicated non-linear function and in principle it is hard or even impossible to find inverse function $G^{-1}(\Theta)$ analytically. Merlet [4] reported the methodology which solves the direct kinematic problem of the parallel SWM. This method is based on the decomposition to the equivalent 3-RS[8] parallel manipulator with revolute joint axes having a common point. Then the direct kinematic problem of the equivalent 3-RS parallel manipulator leads to the solution of a polynomial of order 16 which may only be solved numerically.

In the other hand, the linear dependence between joint actuated velocities $\frac{d}{dt}\Theta$ and the time derivatives of the XYZ Euler's angles $\frac{d}{dt}X$, see (19), makes possible the following.

Suppose the difference e between the measured actuated joint coordinates Θ_m and the recomputed actuated joint coordinates Θ from the computed (estimated) generalized coordinates X, see (27).

Let

$$e = \Theta_m - \Theta = \Theta_m - G\left(X\right) \tag{28}$$

is the expression of such difference. The time derivative of error (28) with a consideration of (19) is

$$\frac{d}{dt}e = \frac{d}{dt}\Theta_m - J^{-1}\left(X\right) \cdot \frac{d}{dt}X \tag{29}$$

The relation (29) gives a differential equation, which describes difference evolution over time. Now, it is necessary to choose a relation between $\frac{d}{dt}e$ and X that ensures convergence of the difference to zero. Assume a choice

$$\frac{d}{dt}e = \frac{d}{dt}\Theta_m - J^{-1}\left(X\right) \cdot \frac{d}{dt}X \stackrel{!}{=} -K\left[\Theta_m - G\left(X\right)\right] = -K \cdot e \tag{30}$$

that leads to linear system

$$\frac{d}{dt}e + Ke = 0 \tag{31}$$

If K is a positive definite matrix, the linear system (31) is asymptotically stable. Consequently, the difference e converges to zero, the recomputed actuated joint coordinates Θ converge to the measurement joint coordinates Θ_m and the computed generalized coordinates X converge to the actual orientation of the end-effector. Suppose that the inverse jacobian $J^{-1}\left(X\right)$ is nonsingular for all positions X of the end-effector through the whole workspace[9]. Consequently, the final dynamic system solving the direct kinematics can be obtained from (30):

$$\frac{d}{dt}X = J\left(X\right)\left[\frac{d}{dt}\Theta_m + K\left[\Theta_m - G\left(X\right)\right]\right] \tag{32}$$

3 Workspace

As it has been mentioned earlier the workspace of the parallel manipulators is more complex than the workspace of the serial manipulator. Thus it is very important to know how the workspace of the manipulator looks like before the manipulator will be manufactured. It is worth noticing that the determination of the workspace is very important task for optimal design of the manipulator.

The definition of the *orientation workspace* of the parallel SWM includes two main parts (**mechanical constraints** and **workspace quality requirements**). We can say that the end-effector orientation X of the parallel SWM belong to the orientation workspace if

[8] 3-RS manipulator consists of 3 independent kinematic chains, each of these chains consists of a link which is connected to the base by the revolute joint (R) and to the end-effector by the spherical joint (S).

[9] Parallel SWM has not any parallel singular positions in its workspace. It has to be ensured by a design of the manipulator.

- the extension of the actuators, the slope angle at the universal joints (C_i) and spherical joints (D_i, E) and the minimal distances between the links $\overrightarrow{C_iD_i}$, $\overrightarrow{OE}$ lie within a given interval $\Rightarrow$ **mechanical constraints**

- the local dexterity index η is grater than a given threshold $\Rightarrow$ **workspace quality requirements**

■ **Note 2 (Local dexterity index)**
The local dexterity index η defines the "distance" which tells us how "far" the orientation X of the end-effector is from the parallel singular position. The local dexterity index $\eta(X,\,\xi)$ for the end-effector orientation X and given design parameters ξ may be defined as

$$\begin{aligned} \eta(X,\,\xi) &= \frac{1}{\mathrm{cond}(J^{-1}(X))} = \frac{\sigma_{min}(J^{-1}(X))}{\sigma_{max}(J^{-1}(X))} \\ \eta(X,\,\xi) &\in \langle 0,\,1\rangle \end{aligned} \tag{33}$$

where $\mathrm{cond}(J^{-1}(X))$ is the condition number of the inverse jacobian and $\sigma_{min}(J^{-1}(X))$ and $\sigma_{max}(J^{-1}(X))$ are the minimal and maximal singular values of the inverse jacobian respectively. It is clear that $\eta(X,\,\xi) = 0$ for the parallel SWM to be at the parallel singular position. Notice that the inverse jacobian will be heterogenous as far as units are concerned. It can be simply seen that the elements of the inverse jacobian of the parallel SWM are lengths. Therefore the local dexterity index $\eta(X,\,\xi)$ is a good singular measurement. ■

Then the orientation workspace W of the parallel SWM for given design parameters ξ is defined as

$$\begin{aligned} W = \{X :\; \|G_i(X,\,\xi) - l_0\| &\le \Delta_l^{max},\; i = 1\ldots 3 \\ S_i(X,\,\xi) &\le \delta^{max},\; i = 1\ldots 4 \\ L_i(X,\,\xi) &\ge l^{min},\; i = 1\ldots 6 \\ \eta(X,\,\xi) &\ge \eta^{min}\} \end{aligned} \tag{34}$$

where $G_i(X,\,\xi)$ is the i-th row of the vector function (27), $S_i(X,\,\xi)$ returns the slope angle at the universal joints (C_i) and spherical joints (D_i, E), $L_i(X,\,\xi)$ returns the minimal distances between the links $\overrightarrow{C_iD_i}$, $\overrightarrow{OE}$, see Note 3, l_0 is length of the prismatic actuators at the parallel SWM's home position and constants Δ_l^{max}, δ^{max}, l^{min}, η^{min} are given constraints of the parallel SWM.

■ **Note 3 (Definition of the functions $S_i(X,\,\xi)$ and $L_i(X,\,\xi)$)**
Function $S_i(X,\,\xi)$ returns the slope angle at the universal joints (C_i) and spherical joints (D_i, E), see Fig. 7, and it is defined as

$$\begin{aligned} \cos\delta_i' &= \frac{\left(\overrightarrow{\bar{C}_i\bar{D}_i}\,,\,\overrightarrow{C_iD_i}\right)}{\|\overrightarrow{\bar{C}_i\bar{D}_i}\|\cdot\|\overrightarrow{C_iD_i}\|} = \cos\delta_i'' = \frac{\left(\overrightarrow{\bar{D}_i\bar{C}_i}\,,\,\overrightarrow{D_iC_i}\right)}{\|\overrightarrow{\bar{D}_i\bar{C}_i}\|\cdot\|\overrightarrow{D_iC_i}\|} = \cos\delta_i \\ \Rightarrow S_i(X,\,\xi) &= \delta_i = \arccos\frac{\left(\overrightarrow{\bar{C}_i\bar{D}_i}\,,\,\overrightarrow{C_iD_i}\right)}{\|\overrightarrow{\bar{C}_i\bar{D}_i}\|\cdot\|\overrightarrow{C_iD_i}\|},\quad i = 1\ldots 3 \\ S_4(X,\,\xi) &= \delta_4 = \arccos\frac{\left(\begin{bmatrix} 0 & 0 & 1 \end{bmatrix}^T,\, R\cdot\begin{bmatrix} 0 & 0 & 1 \end{bmatrix}^T\right)}{\|\overrightarrow{OE}\|}, \end{aligned} \tag{35}$$

where bar denotes the vectors of the parallel SWM in a home position ($X = \overrightarrow{0}$) and $R = R_e^0(X)$ is rotation matrix (1).

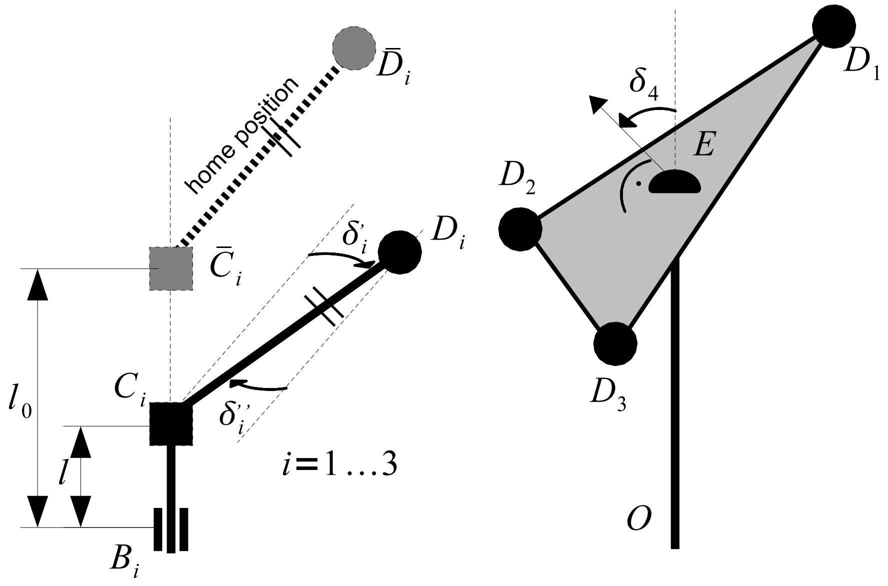

Fig. 7: Definition of the slope angles

The computation of the minimal distance $\mathrm{Dist}(\overrightarrow{AB}, \overrightarrow{CD})$ between two vectors $\overrightarrow{AB}$ and $\overrightarrow{CD}$ has the following possibilities.

1. The minimal distance $\mathrm{Dist}(\overrightarrow{AB}, \overrightarrow{CD})$ between two vectors $\overrightarrow{AB}$ and $\overrightarrow{CD}$ is the norm of the vector $\overrightarrow{X_1X_2}$ which is perpendicular to $\overrightarrow{AB}$ and $\overrightarrow{CD}$ and for which holds $X_1 \in \overrightarrow{AB}$ and $X_2 \in \overrightarrow{CD}$. The points X_1 and X_2 can be written in the parametric form with the parameters $k_1 \in \langle 0,\, 1\rangle$ and $k_2 \in \langle 0,\, 1\rangle$ as

$$\begin{aligned} X_1(k_1) &= A + k_1(B - A) \\ X_2(k_2) &= C + k_2(D - C) \end{aligned} \tag{36}$$

Now we want to find the parameters k_1 and k_2 which minimize $\|\overrightarrow{X_1(k_1)X_2(k_2)}\|$. So the necessary condition have to be satisfied

$$\begin{aligned} \frac{\partial\|\overrightarrow{X_1(k_1)X_2(k_2)}\|^2}{\partial k_1} &= 0 \\ \frac{\partial\|\overrightarrow{X_1(k_1)X(k_2)}\|^2}{\partial k_2} &= 0 \end{aligned} \tag{37}$$

Solution of the equations (37) leads to the system of linear equations for the unknown k_1, k_2

$$\begin{aligned} k_1 - \frac{(B-A\,,\,D-C)}{\|B-A\|^2}k_2 &= -\frac{(A-C\,,\,B-A)}{\|B-A\|^2} \\ k_2 - \frac{(B-A\,,\,D-C)}{\|D-C\|^2}k_1 &= \frac{(A-C\,,\,D-C)}{\|D-C\|^2} \end{aligned} \tag{38}$$

$$\Rightarrow \mathrm{Dist}(\overrightarrow{AB}, \overrightarrow{CD}) = \|\overrightarrow{X_1(k_1)X_2(k_2)}\|$$

2. For $k_1 \notin \langle 0,\, 1\rangle$ or $k_2 \notin \langle 0,\, 1\rangle$. There are four possibilities:

(a) The distance $\mathrm{Dist}(A, \overrightarrow{CD})$
The point $X_2 \in \overrightarrow{CD}$ can be written in the parametric form with the parameter $\bar{k}_1 \in \langle 0, 1\rangle$

$$X_2(\bar{k}_1) = C + \bar{k}_1(D - C) \tag{39}$$

We want to find the parameter $\bar{k}_1$ which minimize $\|\overrightarrow{AX_2(\bar{k}_1)}\|$. So the necessary condition have to be satisfied

$$\frac{\partial\|\overrightarrow{AX(\bar{k}_1)}\|^2}{\partial\bar{k}_1} = 0 \tag{40}$$

The solution of the equation (40) gives

$$\bar{k}_1 = \frac{(A - C\,,\, D - C)}{\|D - C\|^2} \tag{41}$$

$\Rightarrow \mathrm{Dist}(A, \overrightarrow{CD}) = \|\overrightarrow{AX_2(\bar{k}_1)}\| = \mathrm{Di}^{(1)}$
And analogously.

(b) The distance $\mathrm{Dist}(B, \overrightarrow{CD})$
The point $X_2 \in \overrightarrow{CD}$ can be written in the parametric form with the parameter $\bar{k}_2 \in \langle 0, 1\rangle$

$$X_2(\bar{k}_2) = C + \bar{k}_2(D - C) \tag{42}$$

$$\bar{k}_2 = \frac{(B - C\,,\, D - C)}{\|D - C\|^2} \tag{43}$$

$\Rightarrow \mathrm{Dist}(B, \overrightarrow{CD}) = \|\overrightarrow{BX_2(\bar{k}_2)}\| = \mathrm{Di}^{(2)}$

(c) The distance $\mathrm{Dist}(C, \overrightarrow{AB})$
The point $X_1 \in \overrightarrow{AB}$ can be written in the parametric form with the parameter $\bar{k}_3 \in \langle 0, 1\rangle$

$$X_1(\bar{k}_3) = A + \bar{k}_3(B - A) \tag{44}$$

$$\bar{k}_3 = \frac{(C - A\,,\, B - A)}{\|B - A\|^2} \tag{45}$$

$\Rightarrow \mathrm{Dist}(C, \overrightarrow{AB}) = \|\overrightarrow{CX_1(\bar{k}_3)}\| = \mathrm{Di}^{(3)}$

(d) The distance $\mathrm{Dist}(D, \overrightarrow{AB})$
The point $X_1 \in \overrightarrow{AB}$ can be written in the parametric form with the parameter $\bar{k}_4 \in \langle 0, 1\rangle$

$$X_1(\bar{k}_4) = A + \bar{k}_4(B - A) \tag{46}$$

$$\bar{k}_4 = \frac{(D - A\,,\, B - A)}{\|B - A\|^2} \tag{47}$$

$\Rightarrow \mathrm{Dist}(D, \overrightarrow{AB}) = \|\overrightarrow{DX_1(\bar{k}_4)}\| = \mathrm{Di}^{(4)}$

$$\Rightarrow \mathrm{Dist}(\overrightarrow{AB}, \overrightarrow{CD}) = \min_{\forall n:\, \bar{k}_n \in \langle 0, 1\rangle} (Di^{(n)},\ \|\overrightarrow{AD}\|, \|\overrightarrow{AC}\|, \|\overrightarrow{BD}\|, \|\overrightarrow{BC}\|)$$

Function $L_i(X,\,\xi)$ returns the minimal distances between the links $\overrightarrow{C_iD_i}$, $\overrightarrow{OE}$ and it is defined as

$$
\begin{aligned}
L_1(X,\,\xi) &= \mathrm{Dist}(\overrightarrow{C_1D_1},\,\overrightarrow{C_2D_2}) \\
L_2(X,\,\xi) &= \mathrm{Dist}(\overrightarrow{C_1D_1},\,\overrightarrow{C_3D_3}) \\
L_3(X,\,\xi) &= \mathrm{Dist}(\overrightarrow{C_2D_2},\,\overrightarrow{C_3D_3}) \\
L_4(X,\,\xi) &= \mathrm{Dist}(\overrightarrow{C_1D_1},\,\overrightarrow{EO}) \\
L_5(X,\,\xi) &= \mathrm{Dist}(\overrightarrow{C_2D_2},\,\overrightarrow{EO}) \\
L_6(X,\,\xi) &= \mathrm{Dist}(\overrightarrow{C_3D_3},\,\overrightarrow{EO})
\end{aligned}
\tag{48}
$$

■

Merlet [4] reported three basic methods for determining workspace of the parallel manipulators:

geometrical methods: These methods determine geometrically the boundary of the workspace of the manipulator. Notice that geometrical methods are convenient for the translation workspace for which the possible position of the end-effector is given by the intersection of geometrical objects which are parameterized by the design parameters of the manipulator and the constraints of the actuators. The main drawback of the geometrical methods is that it may be difficult to take complex constraints (for an example, see (34)) into account. Therefore we will not deal further with the geometrical methods.

discretization methods: In this approach the workspace is covered by a regular grid of nodes and then each of the nodes is tested to determine whether it belongs to the workspace.

numerical methods: Many of the numerical methods have been proposed recently. For an example, Merlet [3] published methods for determining 6 degrees of freedom workspace of the Gough platform based on interval analysis. Wang et. al. [5] presented a new numerical method based on stratified boundary search technique (SWBDM - Stratified Workspace Boundary Determining Methodology) for determining the translation workspace of the linear delta parallel manipulator and planar Steward platform.

3.1 Discretization method for determining the orientation workspace of the parallel SWM

We suppose the angle $\gamma = \hat{\gamma}$ (rotation of the end-effector about Z axis), where $\hat{\gamma}$ is a constant parameter. So we can cover the plane $\alpha\beta$ by the $N \times N$ rectangular grid[10]. Let $\alpha \in \langle \alpha_{min},\,\alpha_{max}\rangle$, $\beta \in \langle \beta_{min},\,\beta_{max}\rangle$ and the length of the rectangle's sides $\epsilon_\alpha = (\alpha_{max} - \alpha_{min})/(N-1)$, $\epsilon_\beta = (\alpha_{max} - \alpha_{min})/(N-1)$.

So the node $X_{i,j} = \left[\begin{array}{ccc} \alpha_i & \beta_j & \hat{\gamma} \end{array}\right]^T$, where

$$
\begin{aligned}
\alpha_i &= \alpha_{min} + i \cdot \epsilon_\alpha, \quad i = 0 \ldots N-1 \\
\beta_j &= \beta_{min} + j \cdot \epsilon_\beta, \quad j = 0 \ldots N-1,
\end{aligned}
$$

belongs to the orientation workspace if it satisfies the definition (34). Note that a set of the nodes $X_{i,j}$ which satisfy (34) is called *the layer of the orientation workspace for* $\gamma = \hat{\gamma}$. Fig. 8 and Fig. 9 show the orientation workspace for different values of the $\hat{\gamma}$. The design parameters $\xi = \left[\begin{array}{cccc} 1 & 0.6 & 1.3 & 0.3 \end{array}\right]^T$ and $\alpha \in \langle -\pi/2,\,\pi/2\rangle$, $\beta \in \langle -\pi/2,\,\pi/2\rangle$.

[10] A grid formed by tiling the plane regularly with rectangles.

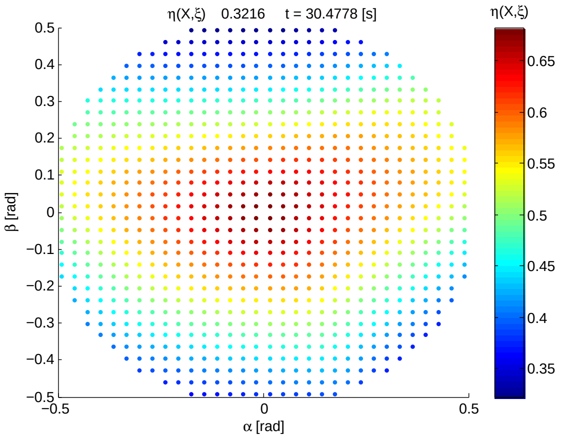

(a) $\hat{\gamma} = 0[rad]$

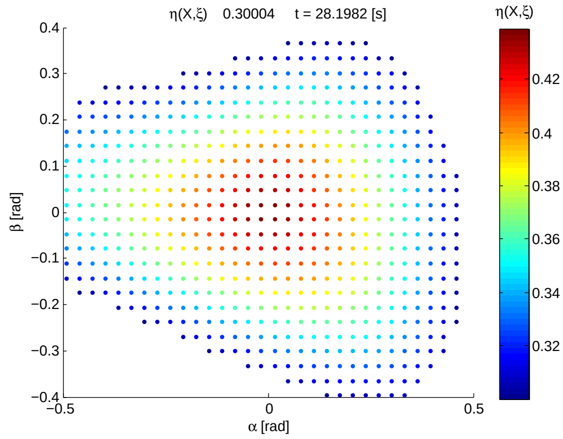

(b) $\hat{\gamma} = 0.5[rad]$

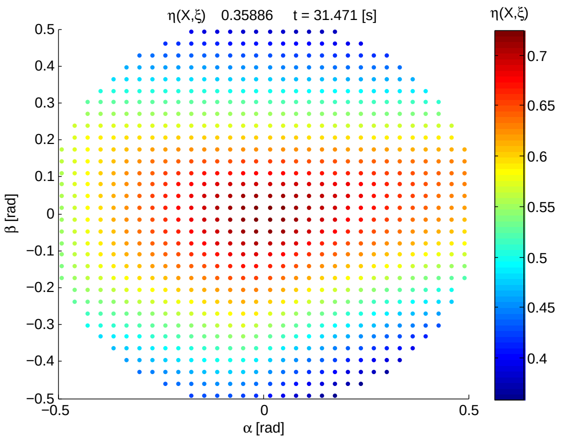

(c) $\hat{\gamma} = -0.5[rad]$

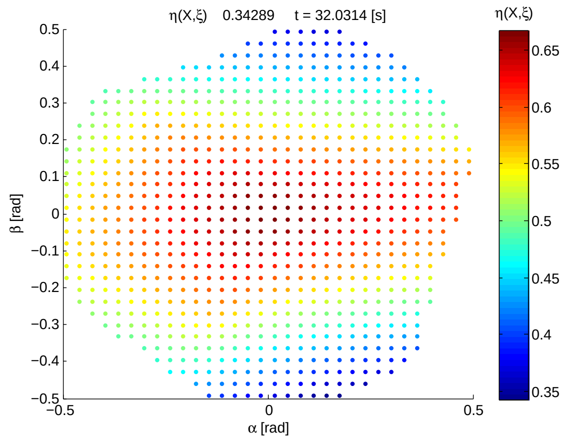

(d) $\hat{\gamma} = -0.8[rad]$

Fig. 8: Workspace of the parallel SWM (discretization method $N = 100 \Rightarrow \epsilon_\alpha = \epsilon_\beta \doteq 0.0317$) for the constraints $\Delta_l^{max} = 0.3[m]$, $\delta^{max} = \pi/6[rad]$, $l^{min} = 0.05[m]$, $\eta^{min} = 0.3$.

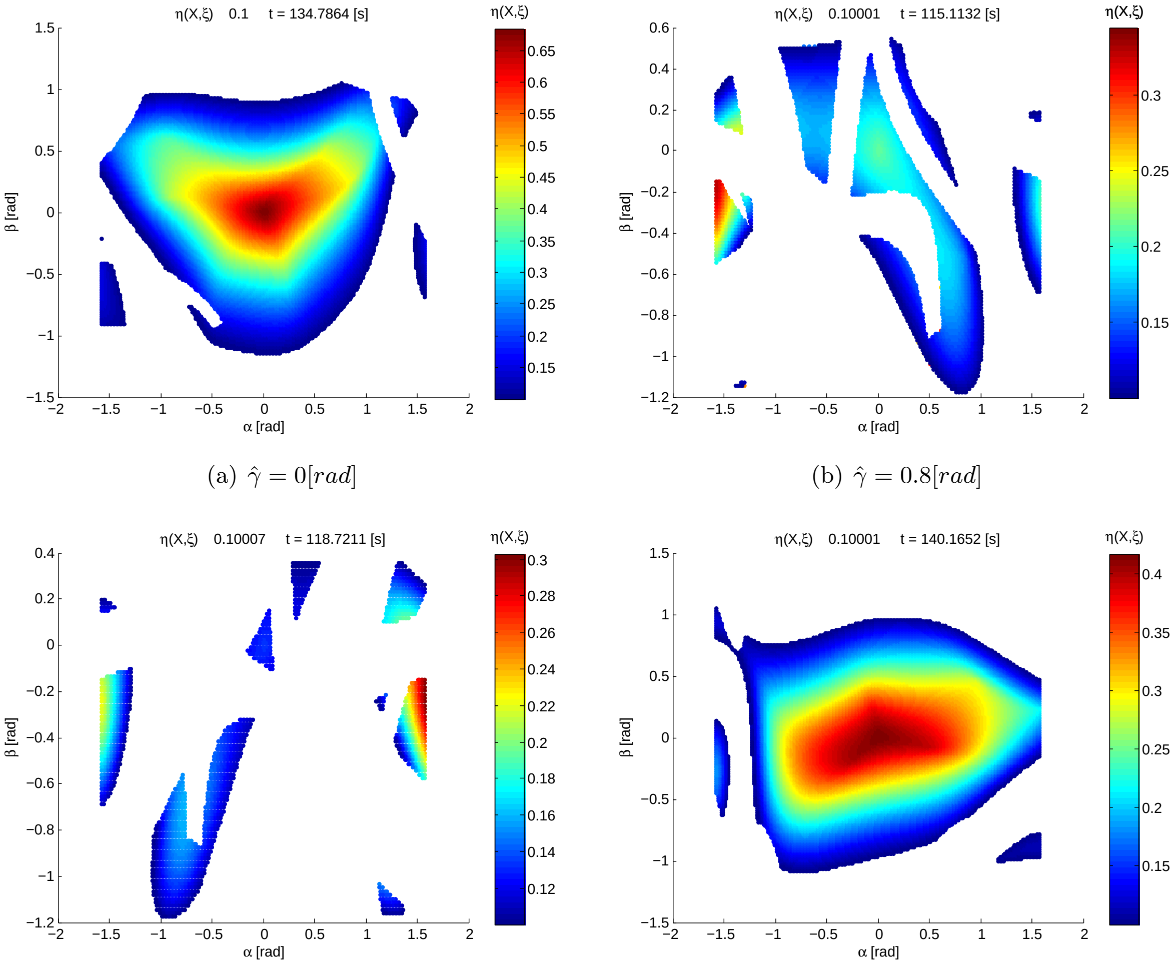

(a) $\hat{\gamma} = 0[rad]$

(b) $\hat{\gamma} = 0.8[rad]$

(c) $\hat{\gamma} = 1,2[rad]$

(d) $\hat{\gamma} = -1.4[rad]$

Fig. 9: Workspace of the parallel SWM (discretization method, $N = 200 \Rightarrow \epsilon_\alpha = \epsilon_\beta \doteq 0.0158$) for the constraints $\Delta_l^{max} = 0.5[m]$, $\delta^{max} = \pi/2[rad]$, $l^{min} = 0.03[m]$, $\eta^{min} = 0.1$.

Advantages and disadvantages of this approach:

+ Easy realization.

+ Complex constraints of the orientation workspace, similar to (34), can be taken into account.

- We need a large number of evaluations of the constraints (34) for a high accuracy (small discretization step ϵ_α, ϵ_β) which leads to high time consuming algorithm (computation time t, see Fig. 8 and Fig. 9).

3.2 SWBDMD for determining the orientation workspace of the parallel SWM

In this section we apply the modified SWBDM [5] in order to determine the orientation workspace boundary of the parallel SWM and calculate the size (volume) of this workspace. Contrary to the discretization method mentioned above the SWBDM is based on an idea not to test all points (nodes) of the given grid but to search and test only a few points around the workspace boundary.

■ Note 4 (Determination of the workspace layer area)
If we consider workspace layer $\alpha\beta$ (for a fixed values of $\gamma = \hat{\gamma}$). Its area can be determined (with the help of knowledge about the workspace boundary points $\hat{X}^{(k)}_{\alpha,\beta}$) as a sum of the triangle areas, see Fig. 10.

$$S_{\hat{\gamma}} = \sum_{k=1}^{N-1} \sqrt{s^{(k)}(s^{(k)} - l_1^{(k)})(s^{(k)} - l_2^{(k)})(s^{(k)} - l_3^{(k)})}, \tag{49}$$

where $l_1^{(k)} = \|\hat{X}^{(k)}_{\alpha,\beta} - X_c\|$, $l_2^{(k)} = \|\hat{X}^{(k+1)}_{\alpha,\beta} - X_c\|$, $l_3^{(k)} = \|\hat{X}^{(k+1)}_{\alpha,\beta} - \hat{X}^{(k)}_{\alpha,\beta}\|$, $s^{(k)} = (l_1^{(k)} + l_2^{(k)} + l_3^{(k)})/2$ and N is the number of the workspace boundary points

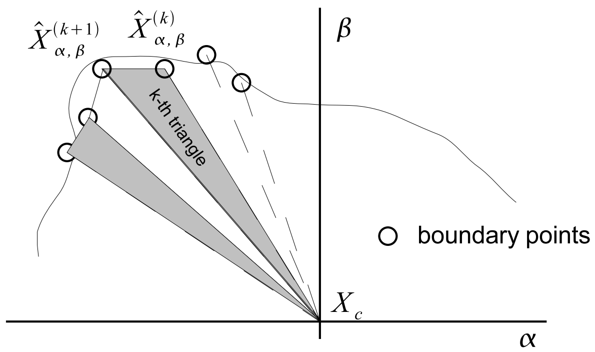

Fig. 10: Workspace boundary points and area of the layer $\alpha\beta$, $\gamma = \hat{\gamma}$

■

The basic algorithm for the workspace layer $\alpha\beta$ (for a fixed values of $\gamma = \hat{\gamma}$) is

♦ **Algorithm 1 (Determination of the workspace boundary layer $\alpha\beta$, $\gamma = \hat{\gamma}$)**

1. Define so-called central point $X_c = \begin{bmatrix} \alpha & \beta & \hat{\gamma} \end{bmatrix}^T$ which always satisfies $X_c \in W$ {1}[11]

2. Define a positive real number ϵ as a neighborhood radius and suppose the neighborhood of the point $X_{\alpha,\beta} = [\alpha,\ \beta,\ \hat{\gamma}]$ as

$$\begin{aligned} X_{\alpha,\beta,1} &= X_{\alpha,\beta} + \begin{bmatrix} \epsilon & 0 & 0 \end{bmatrix}^T, \quad X_{\alpha,\beta,2} = X_{\alpha,\beta} + \begin{bmatrix} 0 & \epsilon & 0 \end{bmatrix}^T, \\ X_{\alpha,\beta,3} &= X_{\alpha,\beta} + \begin{bmatrix} -\epsilon & 0 & 0 \end{bmatrix}^T, \quad X_{\alpha,\beta,4} = X_{\alpha,\beta} + \begin{bmatrix} 0 & -\epsilon & 0 \end{bmatrix}^T \end{aligned} \tag{50}$$

   Then we can say that the point $X_{\alpha,\beta}$ is an *interior point* of the workspace if **all the points** in (50) lie in the interior of the workspace (satisfy (34)). The point $X_{\alpha,\beta}$ is an *exterior point* of the workspace if **all the points** in (50) do not lie in the interior of the workspace. Otherwise the point $X_{\alpha,\beta}$ is a *boundary point* of the workspace.

3. Determine the first boundary point $\hat{X}^{(1)}_{\alpha,\beta}$ of the workspace layer. {2}

   (a) Let $j = 1$, $X^{(j)}_{\alpha,\beta} = X_c + \begin{bmatrix} 2\epsilon & 0 & 0 \end{bmatrix}^T$ is a starting point of the layer.

   (b) **if**
   $X^{(j)}_{\alpha,\beta}$ is the interior point *and* $X^{(j-1)}_{\alpha,\beta}$ is not the exterior point[12]
   then
   $X^{(j+1)}_{\alpha,\beta} = X^{(j)}_{\alpha,\beta} + 2\epsilon \frac{X^{(j)}_{\alpha,\beta} - X_c}{\|X^{(j)}_{\alpha,\beta} - X_c\|}$, $j = j + 1$ and goto 3b

[11]{1}...{6} denote the step of the SWBDM, see Fig. 11.
[12]For $j = 0$ the condition "$X^{(j-1)}_{\alpha,\beta}$ is not the exterior (or interior) point" is considered to be satisfied.

else if
$X^{(j)}_{\alpha,\beta}$ is the exterior point *and* $X^{(j-1)}_{\alpha,\beta}$ is not the interior point *and* $\|X^{(j)}_{\alpha,\beta} - X_c\| > 2\epsilon$
then
$X^{(j+1)}_{\alpha,\beta} = X^{(j)}_{\alpha,\beta} - 2\epsilon\frac{X^{(j)}_{\alpha,\beta}-X_c}{\|X^{(j)}_{\alpha,\beta}-X_c\|}$, $j = j+1$ and goto 3b
else ($X^{(j)}_{\alpha,\beta}$ is the boundary point)
$\hat{X}^{(1)}_{\alpha,\beta} = X^{(j)}_{\alpha,\beta}$

4. Determine the boundary points $\hat{X}^{(k)}_{\alpha,\beta}$ of the workspace

   (a) $k = 1$, $j = 1$, $X^{(j)}_{\alpha,\beta} = \hat{X}^{(k)}_{\alpha,\beta} + \begin{bmatrix} 0 & 2\epsilon & 0 \end{bmatrix}^T$ (the first search direction along workspace boundary) {3}

   (b) **if**
   $X^{(j)}_{\alpha,\beta}$ is the interior point *and* $X^{(j-1)}_{\alpha,\beta}$ is not the exterior point
   then
   $X^{(j+1)}_{\alpha,\beta} = X^{(j)}_{\alpha,\beta} + 2\epsilon\frac{X^{(j)}_{\alpha,\beta}-X_c}{\|X^{(j)}_{\alpha,\beta}-X_c\|}$, $j = j+1$ and goto 4b {6}
   else if
   $X^{(j)}_{\alpha,\beta}$ is the exterior point *and* $X^{(j-1)}_{\alpha,\beta}$ is not the interior point *and* $\|X^{(j)}_{\alpha,\beta} - X_c\| > 2\epsilon$
   then
   $X^{(j+1)}_{\alpha,\beta} = X^{(j)}_{\alpha,\beta} - 2\epsilon\frac{X^{(j)}_{\alpha,\beta}-X_c}{\|X^{(j)}_{\alpha,\beta}-X_c\|}$, $j = j+1$ and goto 4b {5}
   else if ($X^{(j)}_{\alpha,\beta}$ is the boundary point)
   $\|X^{(j)}_{\alpha,\beta} - \hat{X}^{(1)}_{\alpha,\beta}\| > 2\epsilon$ *or* $k \leq 5$ [13]
   then
   $\hat{X}^{(k+1)}_{\alpha,\beta} = X^{(j)}_{\alpha,\beta}$,
   $j = 1$,
   $X^{(j)}_{\alpha,\beta} = \hat{X}^{(k)}_{\alpha,\beta} + 2\epsilon\frac{\hat{X}^{(k+1)}_{\alpha,\beta}-\hat{X}^{(k)}_{\alpha,\beta}}{\|\hat{X}^{(k+1)}_{\alpha,\beta}-\hat{X}^{(k)}_{\alpha,\beta}\|}$ (the next search direction along the workspace boundary), {4}
   $S_{\hat{\gamma}} = S_{\hat{\gamma}} + \sqrt{s^{(k)}(s^{(k)} - l^{(k)}_1)(s^{(k)} - l^{(k)}_2)(s^{(k)} - l^{(k)}_3)}$ (k-th triangle area, see Note 4),
   $k = k+1$ and goto 4b
   else
   Determination of the workspace boundary points is completed for the layer $\alpha\beta$, $\gamma = \hat{\gamma}$.
   Stop the algorithm.

♦

Fig. 11 shows a principle of the SWBDM which is given by the Algorithm 1.

[13] Minimal number of the workspace boundary points is 5.

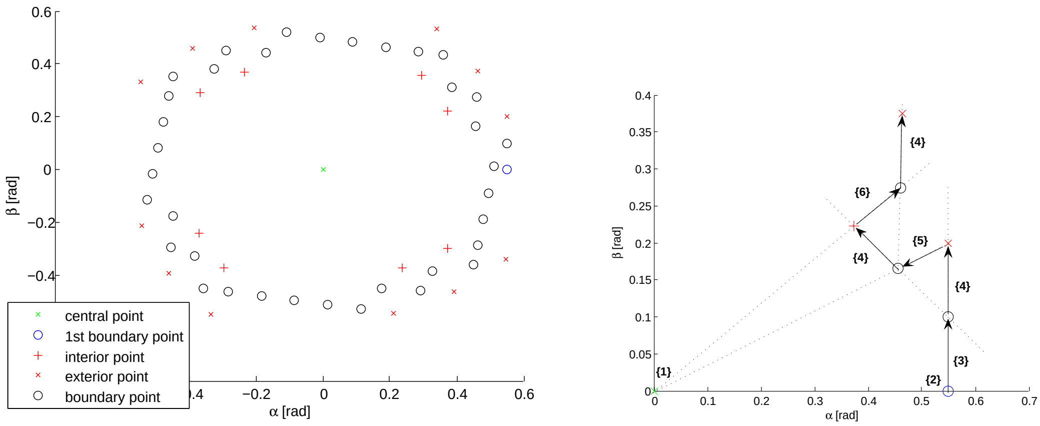

(a) Boundary of the workspace

(b) Zoom and description of steps of the Algorithm 1

Fig. 11: Principle of the SWBDM

Now we use SWBDM (central point $X_c = \begin{bmatrix} 0 & 0 & \hat{\gamma} \end{bmatrix}^T$) for a determining the orientation workspace of the parallel SWM with the same design parameters ξ and constraints of the workspace Δ_l^{max}, δ^{max}, l^{min}, η^{min} as in Fig. 8 and Fig. 9. Note that the neighborhood radius ϵ approximately corresponding to the grid accuracy $\epsilon_\alpha = \epsilon_\beta$ (quadratic grid in section 3.1) can be evaluate as $\epsilon = \frac{\alpha_{max}-\alpha_{min}}{2(N-1)}$. Fig. 12 and Fig. 13 show a comparison of the orientation workspace boundary (SWBDM) to orientation workspace (discretization method in section 3.1).

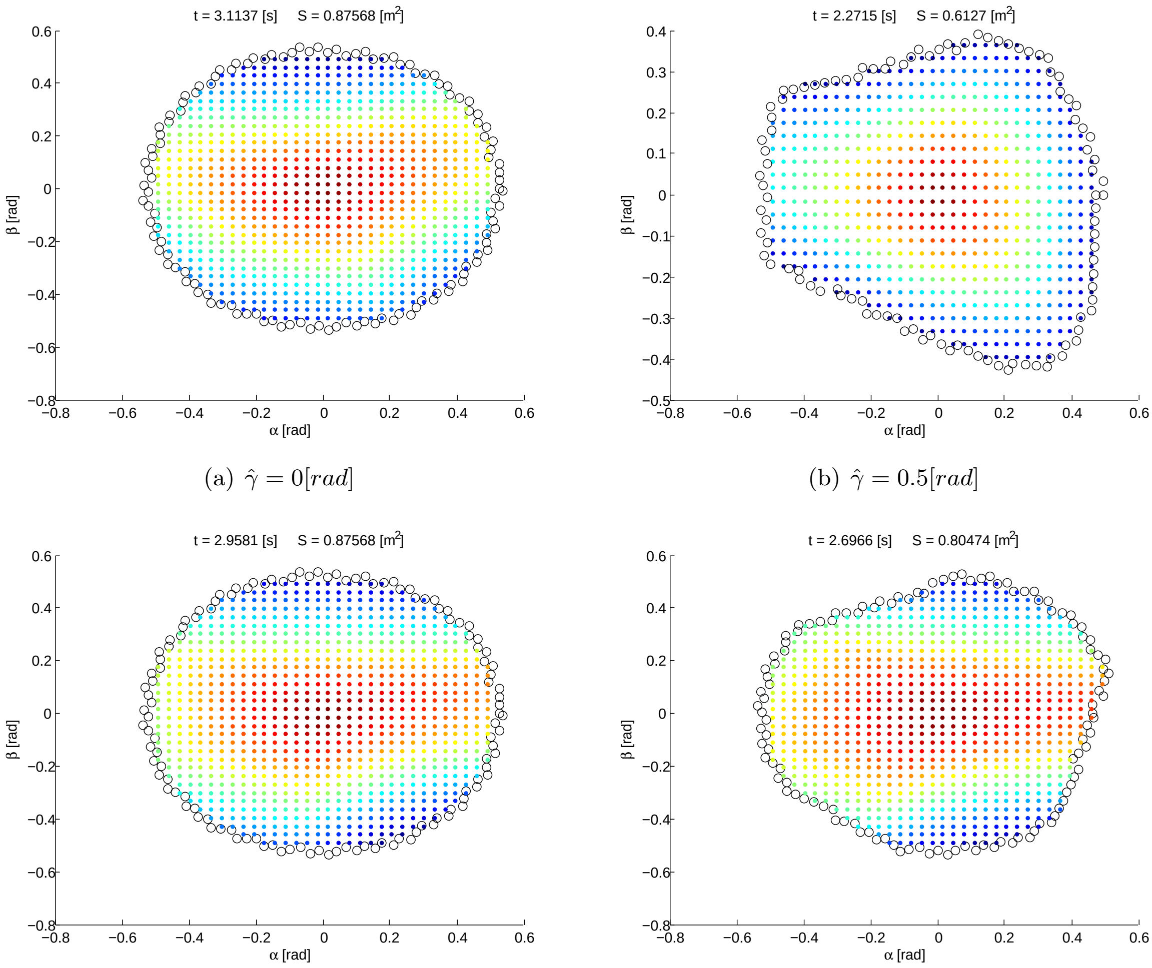

(a) $\hat{\gamma} = 0[rad]$

(b) $\hat{\gamma} = 0.5[rad]$

(c) $\hat{\gamma} = -0.5[rad]$

(d) $\hat{\gamma} = -0.8[rad]$

Fig. 12: Workspace of the parallel SWM (SWBDM, $\epsilon \doteq 0.0159$) for the constraints $\Delta_l^{max} = 0.3[m]$, $\delta^{max} = \pi/6[rad]$, $l^{min} = 0.05[m]$, $\eta^{min} = 0.3$.

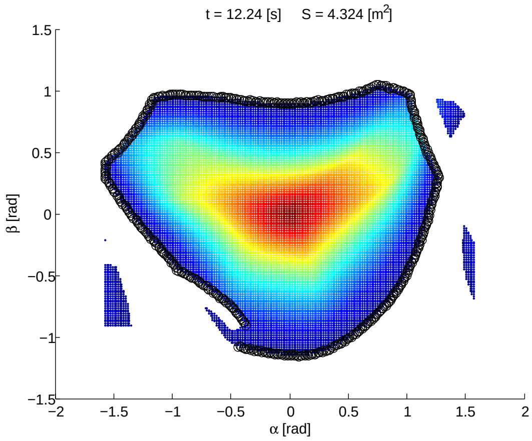

(a) $\hat{\gamma} = 0[rad]$

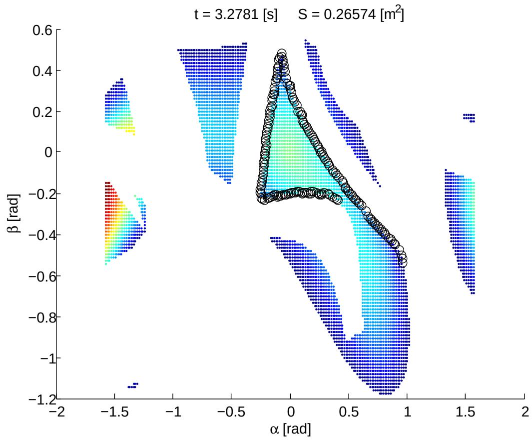

(b) $\hat{\gamma} = 0.8[rad]$

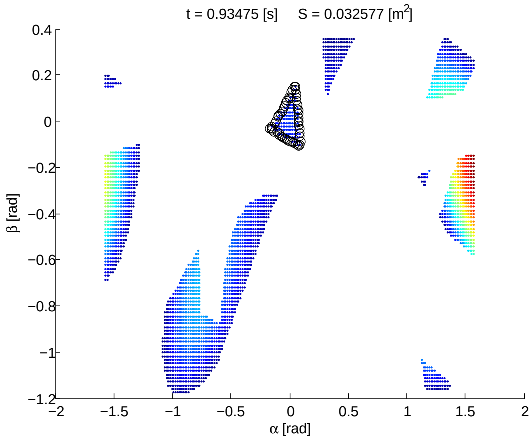

(c) $\hat{\gamma} = 1,2[rad]$

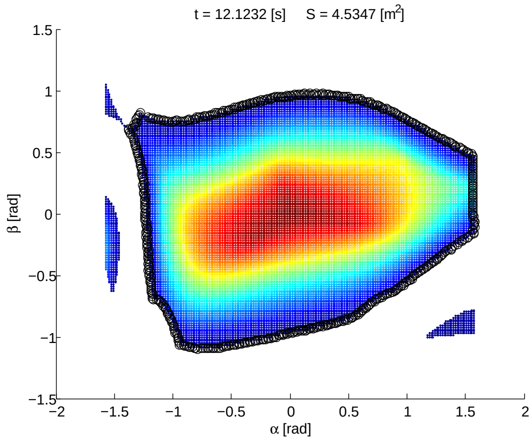

(d) $\hat{\gamma} = -1.4[rad]$

Fig. 13: Workspace of the parallel SWM (SWBDM, $\epsilon \doteq 0.0079$) for the constraints $\Delta_l^{max} = 0.5[m]$, $\delta^{max} = \pi/2[rad]$, $l^{min} = 0.03[m]$, $\eta^{min} = 0.1$.

Advantages and disadvantages of this approach:

+ very fast algorithm in comparison with the discretization methods, see Tab. 1

accuracy	$\epsilon_\alpha = \epsilon_\beta = 0.0317$, $\epsilon = 0.0159$				$\epsilon_\alpha = \epsilon_\beta = 0.0158$, $\epsilon = 0.0079$			
layer $\gamma[rad]$	-0.8	-0.5	0	0.5	-1.4	0	0.8	1.2
method	computation time t [s]							
dicretization method	32.03	31.47	30.48	28.20	140.17	134.79	115.11	118.72
SWBDM	2.70	2.96	3.11	2.27	12.12	12.24	3.28	0.93

Table 1: Time consuming comparison between the proposed methods

- Workspace boundary searching depends on a choice of the central point X_c very much. Therefore this method can not find all of the boundary points for some type of workspaces. Zoom of Fig. 13(a) and Fig. 13(b) shows how SWBDM works for the central point $X_c = \begin{bmatrix} 0 & 0 & \hat{\gamma} \end{bmatrix}^T$, see Fig. 14.

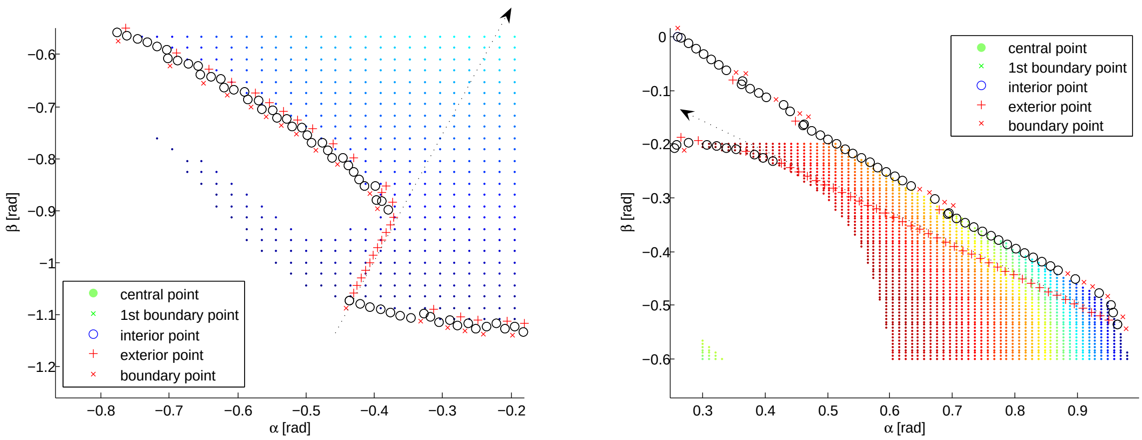

(a) $\hat{\gamma} = 0[rad]$ (b) $\hat{\gamma} = 0.8[rad]$

Fig. 14: The failure of the SWBDM

This disadvantage could be overcome by adapting of the central point position when the length between two consecutive boundary points exceed a given threshold. But generally, the SWBDM gives the very fast algorithm searching only an **approximation** of the workspace boundary.

- SWBDM can not deal with workspaces with voids, see Fig. 13.

4 Conclusion

A basic kinematic study has been proposed for the parallel spherical wrist manipulator (parallel SWM). The inverse and forward kinematic problem was solved. Singular positions of the parallel SWM were found and their influence on a control of the manipulator was shown. We used two methods for determining the parallel SWM workspace (*general dicretization method* and *modified stratified workspace boundary determining methodology (SWBDM)* which was firstly reported in [5]). We could see that the SWBDM can not simply deal with a complex workspace (with voids and complicated shape) but for its low computational load it can be use for determining complete 3D parallel SWM orientation workspace.

If we denote a direction along γ as a stratified direction of the orientation workspace we can divide the 3D orientation workspace into M layers $\alpha\beta$, $\hat{\gamma}_i$, where $\hat{\gamma}_i = \hat{\gamma}_{i-1} + i \cdot 2\epsilon$ and the central point $X_c = \begin{bmatrix} 0 & 0 & \hat{\gamma}_i \end{bmatrix}^T \in W$. Then a volume of the orientation workspace is $V = 2\epsilon \sum_{i=1}^{M} S_{\hat{\gamma}_i}$. Fig. 15 shows complete orientation workspace of the parallel SWM for the design parameters $\xi = \begin{bmatrix} 1 & 0.6 & 1.3 & 0.3 \end{bmatrix}^T$ and for the workspace constraints $\Delta_l^{max} = 0.3[m]$, $\delta^{max} = \pi/6[rad]$, $l^{min} = 0.05[m]$, $\eta^{min} = 0.3$.

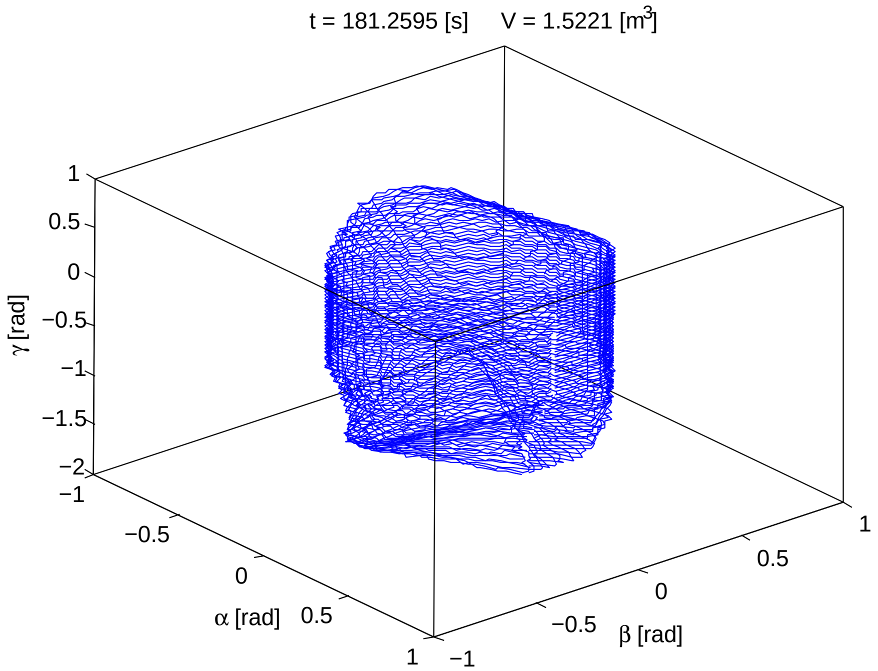

Fig. 15: Complete orientation workspace of the parallel SWM (SWBDM)

References

[1] B. Siciliano L. Sciavicco. *Modelling and Control of Robot Manipulators.* Springer, 2000.

[2] The MathWorks. *SimMechanics User's Guide, www.mathworks.com.*

[3] J-P. Merlet. Determination of 6d-workspaces of gough-type parallel manipulator and comparison between different geometries. *INRIA Sophia-Antipolis, France.*

[4] J. P. Merlet. *Parallel robots.* Springer, 2006.

[5] J. Sun Ch. Ou Y. Wan Z. Wang, S. Ji. A methodology for determining the reachable and dexterous workspace of parallel manipulators. *International Conference on Mechatronics and Automation, Proceedings of the 2007 IEEE*, 2007.